

RESEARCH ARTICLE

The behavior of ternary hybrid nanofluid: Graphene oxide, Aluminium oxide, and Silicon dioxide in heat transfer rate

F. M. Hanapiah¹, I. A. Zakaria^{1*}, S. R. Makhsin^{1,2}, N. Hamzan¹

¹ School of Mechanical Engineering, College of Engineering, Universiti Teknologi MARA, 40450, Shah Alam, Selangor, Malaysia
 Phone: +60 3-5543 5052; Fax.: +60 3-5543 5042

² AEH Innovative Hydrogel Ltd, Graphene Engineering Innovation Centre, Sackville St, Manchester M1 3BB, United Kingdom

ABSTRACT - Miniaturization in the design of electronic systems has become inevitable due to the rapid advancement and development of technology. This has imposed challenges to the thermal management capability as the heat flux density has increased tremendously due to a smaller heat transfer surface. Nanofluid adoption in electronic cooling seems to be an alternative way to achieve better heat dissipation. This research explores the feasibility of ternary hybrid nanofluids GO: Al₂O₃: SiO₂ in water with different volume concentrations and mixture ratios in a serpentine cooling plate. In this research, 0.01% GO + Al₂O₃: SiO₂, 0.006% GO + Al₂O₃: SiO₂, and 0.008% GO + Al₂O₃: SiO₂ in mixture ratios of 10:90 and 20:80 (Al₂O₃: SiO₂) were studied. The result showed that 0.01% GO + Al₂O₃: SiO₂ (10:90) nanofluids displayed the highest enhancement of heat transfer coefficient with 1.1 times higher as compared to the base fluid. This was then followed by 0.008% GO + Al₂O₃: SiO₂ (10:90) and 0.006% GO + Al₂O₃: SiO₂ (10:90) with 1.03 times and 0.87 times higher heat transfer coefficient enhancement consecutively as compared to the base fluid. In term of mixture ratios, GO in 10:90 (Al₂O₃: SiO₂) performed better than 20:80. To assess the feasibility of adoption, the advantage ratio (AR) was conducted to measure both heat transfer enhancement and pressure drop effect. The AR analysis showed that at the lower Reynolds, *Re* number region, the 0.01% GO + Al₂O₃: SiO₂ (10:90) ternary hybrid nanofluids was proven to be the most feasible due to a higher ratio of heat transfer enhancement over the pressure drop penalty.

ARTICLE HISTORY

Received : 11th Jan. 2024
 Revised : 23rd Mar. 2024
 Accepted : 24th May 2024
 Published : 28th June 2024

KEYWORDS

Nanofluids
 Ternary Hybrid
 Cooling plate
 Heat transfer
 Pressure drop

1. INTRODUCTION

The world is currently spectating the advancement of technologies that have encouraged further research and development on effective thermal management for cooling methods of compact electrical/electronic devices or systems. Electrical/electronic devices or systems generally consist of electrically powered devices and equipment and any system that generates, distributes, or consumes energy from electricity. As a by-product, these devices or equipment generate immense heat. Thus, the system critically needs to establish an effective cooling system to remove the heat and maintain the efficiency, reliability, and long lifespan of the devices or components. Furthermore, miniaturization in the design of these electrical/electronic devices due to the rapid advancement and development of technology, which requires an increase in speed and power, became unavoidable, posing additional challenges to the thermal management capability as the heat flux per unit area of these devices has increased [1]. As a result, the efficient cooling technique is critical for electrical/electronic devices to improve thermal management without increasing the system size.

In general, several types of cooling approaches for an electrically active environment system can be classified as passive and active cooling methods. Compared to passive cooling, active cooling uses large heat exchangers to enhance heat dissipation, which provides a greater forced convection area for the cooling medium in the system [2]. Therefore, despite having the ability to provide substantial cooling capacity, active cooling is not favored since it demands a greater surface area, which is essential nowadays for electrical system miniaturization. Alternatively, liquid cooling using coolant, a passive method of heat elimination in electrical cooling, is introduced. However, there is a limitation in removing the heat efficiently due to the poor thermal properties of the coolant. Utilizing deionized water as the coolant may be insufficient to satisfy the need for higher cooling rates in smaller system sizes. Furthermore, the thermal reactions of the cooling method using water do not meet the requirement for a uniform temperature distribution throughout the cooling plate [3].

Adopting nanoparticles dispersed in the distilled water, which acts as the base fluid, is expected to provide a better solution for increasing the efficiency of distilled water as the conventional coolant. Adopting nanofluids improves heat transfer, mainly due to the improvement of its thermal conductivity [4, 5]. Sundar et al.[6] reported thermal conductivity enhancement of 9.8 % and 15.6 %, respectively, in Al₂O₃ and CuO nanofluids dispersed in EG and water mixtures. According to Kamel et al.[7], Al₂O₃ nanofluids have improved in thermal conductivity by 5.34 % at 0.5 volume % at 50 °C) compared to the base fluid. Meanwhile, Khalid et al. [8] discovered that SiO₂ nanofluids with 0.5% volume concentration enhanced thermal conductivity by 1.42 % compared to the base fluid. The development of hybrid and

ternary nanofluids is further established to improve nanofluids' characteristics in heat transfer performance. Suresh et al. [9] reported that the heat transfer coefficient of Al_2O_3 -Cu/water hybrid nanofluids flowing in a tube have a Nusselt number boost of 13.56 % at 0.1 % concentration in volume at Reynolds number of 1730. Madhesh et al. [10] studied the Cu-SiO₂/water hybrid nanofluid with 2.0 % volume concentration discovered that the overall heat transfer coefficient and Nusselt number are enhanced by 68 % and 49 %, respectively as compared to water. However, it was also discovered that there is an increase in pumping power by 14.9 % caused by the hybrid nanofluid as compared to the base fluid.

Similarly, Moldoveanu et al. [11, 12] reported the comparative overall viscosity for alumina nanofluids which is higher in comparison to SiO₂ nanofluids. It was also reported that higher volume fractions of SiO₂ nanoparticles placed in studied hybrid nanofluids leads to higher thermal conductivities values. The researchers later established a few correlations for a better estimation of the viscosity and thermal conductivity for Al_2O_3 , SiO₂ water-based nanofluids. Meanwhile, Saifudin et al. [13] developed a performance enhancement ratio (PER) for 0.5 % concentration Al_2O_3 :SiO₂ hybrid nanofluids in both thermal conductivity enhancement over viscosity and electrical conductivity penalty in Proton Exchange Membrane Fuel Cell (PEMFC) cooling application. According to the study, the most feasible 0.5% concentration Al_2O_3 :SiO₂ hybrid nanofluids mixture ratio was 10:90 which has shown relatively good PER as compared to the other mixture. On another note, there is a limited discovery on the heat transfer performance of the ternary hybrid nanofluid in open literature. Among the available studies is by Ramadhan et al. [14], who reported that the heat transfer coefficient for the Al_2O_3 :SiO₂:TiO₂ coolant side is increased by a total of 39.7 % at a volume concentration of 0.3%. In a study by Muzaidi et al. [15], the heat absorption characteristics of CuO: TiO₂:SiO₂ ternary hybrid nanofluids and TiO₂:SiO₂ hybrid nanofluid were compared and highlighted that the ternary hybrid nanofluid outperformed the hybrid nanofluid by a factor of 97.3 %.

This study is a continuity of previous studies on Al_2O_3 :SiO₂ hybrid nanofluids conducted before. The Al_2O_3 and SiO₂ nanoparticles were chosen due to their superior thermal conductivity properties and stability [16]. In addition to that, GO was added to the established Al_2O_3 :SiO₂ hybrid nanofluids conducted before. The GO was prepared in-house and thus is cost economic for the adoption. It is aimed to explicate the characterization, heat transfer, and fluid flow performance and its feasibility of adoption as a newly formed ternary hybrid nanofluids of GO in Al_2O_3 : SiO₂.

2. MATERIALS AND METHODS

2.1 Nanofluids Preparation

As for the nanofluids preparation, the liquid formed SiO₂ nanoparticles with a particle size of 30 nm, a purity of 99.9 % and a weight percentage of 25 weight percentages were procured from Nova Scientific Sdn. Bhd. Meanwhile, the Al_2O_3 nanoparticles were acquired from Sigma Aldrich (M) in powder form, with an average particle size of 13 nm and 99.8 % purity. For the GO, the aqueous solution of GO nanofluid was obtained with a volume concentration of 0.01 %, 0.008 %, and 0.006 %. The two-step method was used for the nanofluid sample preparation as this approach has improved stability, which reduces agglomeration and lowers the risk of oxidation for high thermal conductivity metal particles.

As for the powder form nanoparticle, the volume concentration was determined based on the equation below [8]:

$$\varphi = \frac{\left(\frac{m_p}{\rho_p}\right)}{\left(\frac{m_p}{\rho_p} + \frac{m_{bf}}{\rho_{bf}}\right)} \times 100 \quad (1)$$

where φ is the volume concentration, m is the mass, ρ is the density. Subscripts p and bf represent the nanoparticle and base fluid. For the liquid-form nanoparticles, the dilution is measured by using the following equation [13]:

$$\Delta V = (V_2 - V_1) = V_1 \left(\frac{\varphi_1}{\varphi_2} - 1\right) \quad (2)$$

where ΔV is the volume of base fluid needed to be added, V_1 with a concentration of φ_1 to obtain the desired volume of nanofluid, V_2 with volume concentration, φ_2 .

The diluted nanoparticles for both Al_2O_3 and SiO₂ were then measured and mixed using the magnetic stirrer for 30 minutes to form hybrid nanofluids with two different ratios which were 10:90 and 20:80. Upon completion of the mixing process, the nanofluid solutions were sonicated using Daihan Scientific Ultrasonic Sonicator for two hours to enhance the stability of the solution. The duration for magnetic stirring and ultrasonication were based on best practices by renowned researchers [17, 18]. Once the single nanofluids preparation was completed, the ternary hybrid nanofluids were then prepared for all the mixture ratios required. The 0.01 %, 0.008 % and 0.006 % volume concentration of GO nanofluids were then added to the hybrid mixture ratio samples. The same mixing method and sonication process were applied to prepare the ternary hybrid nanofluids. Figure 1 shows the mixing and sonication process for the nanofluid sample. The properties of nanoparticles and base fluid used in this study are shown in Table 1.

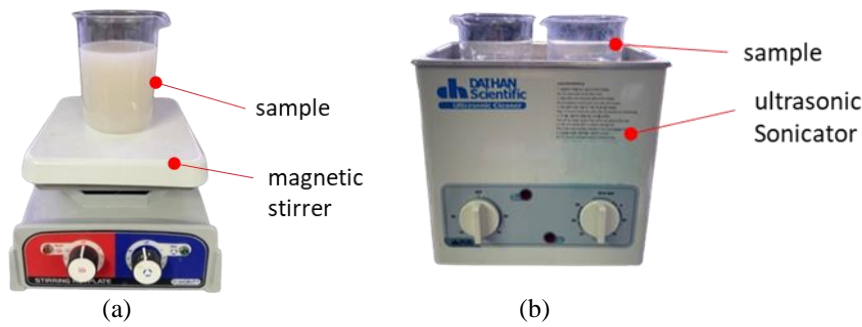


Figure 1. (a) Magnetic stirrer and (b) Ultrasonic sonicator used in preparation process

Table 1. The properties of nanoparticle and base fluid

Elements	Matter Classification	Thermal Conductivity, k (W/mk)	Specific Heat, c_p (J/kg.K)	Viscosity (Pa.s)	Density (kg/m ³)	Reference
GO nanoparticles	Solid	2500-5000	790	-	2000	[19]
Al ₂ O ₃ nanoparticles	Solid	36	765	-	4000	[20]
SiO ₂ nanoparticles	Solid	1.38	745	-	2220	[21]
Water	Liquid	0.615	4180	0.000854	999	[8]

2.2 Stability Measurement

The stability of the prepared ternary hybrid nanofluids was determined using two approaches which are visual observation and Zeta potential analysis. As for visual observation, the sedimentation of the particles in the nanofluids was observed visually for all samples of ternary hybrid nanofluids periodically. Meanwhile, the Zeta potential values of the ternary hybrid nanofluids were analyzed to determine the electro-stability of the nanoparticles dispersed in the base fluid. Litesizer 500 was used to measure the zeta potential of the measured nanofluids.

2.3 Thermophysical Properties Measurement

2.3.1 Thermal conductivity

The thermal conductivity measurement of the nanofluids studied in this research was conducted using the Modified Transient Plane Source from C-Therm which complied with ASTM D7984 standard. This device used the transient line heat source method to enhance the accuracy of thermal conductivity measurement. The device featured a single-sided, interface heat absorbance sensor that applied a constant source of heat to the sample for a brief period. At the location where the sensor and the nanofluid sample made contact, the delivered current caused a temperature increase that caused a change in voltage drop in the sensor element. As the rate of rise in temperature of the sensor element is exactly proportional to the thermal conductivity, the rate of rise in sensor voltage was then calibrated to temperature and utilized to analyze the thermal conductivity of the nanofluids using the C-Therm TCi Thermal Conductivity Analyzer as shown in Figure 2. The measurement of all nanofluid's thermal conductivity was done at room temperature of 30 °C as some research discovered that above 50°C, there will be a higher reading error due to the convective heat transfer effect [10]. Multiple readings were recorded to obtain more accurate data for the thermal conductivity of the nanofluids. The C-Therm was calibrated by measuring the distilled water and the value of thermal conductivity obtained was compared to the known value for the distilled water.



Figure 2. C-Therm TCi thermal conductivity analyzer

2.3.2 Viscosity

The viscosity of the nanofluids sample was measured using the Anton Paar Rheolab QC device as shown in Figure 3. The device was equipped with a rotational rheometer to ensure quality control for the viscosity measurement. The viscosity measuring range for this device is from 1 to 10⁹ mPas. The viscosity of the nanofluids sample was analysed at a temperature range of 30 °C to 80 °C. To ensure reliable data from the viscosity measurement of the nanofluids, multiple

reading was taken and recorded. The device calibration was done by measuring the distilled water and the measurement was compared to the reference value of distilled water.



Figure 3. Anton Paar Rheolab QC device

2.3.3 Electrical conductivity

The measurement of the electrical conductivity of all nanofluid samples was conducted using the EUTECH Handheld Meter Kit PC450 as depicted in Figure 4. The device was equipped with a special DJ PH probe that can be used to measure the electrical conductivity, temperature, and PH value of the liquid solution. The reading of the electrical conductivity was taken at a temperature range from 30 °C to 80 °C. In order to ensure a precise assessment of the electrical conductivity of the nanofluids, multiple readings were taken and recorded. The equipment was calibrated using distilled water and ethylene glycol and the readings were compared against the reference value.

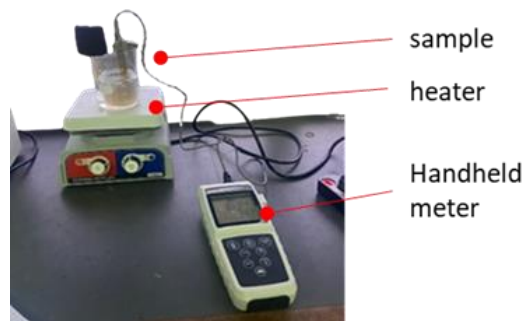


Figure 4. EUTECH handheld meter kit PC450

2.3.4 Numerical model of the serpentine cooling plate

The heat transfer and fluid performance of the ternary hybrids nanofluids in the serpentine cooling plate were simulated using ANSYS Fluent. The geometry of the cooling plate was created using CATIA V5R20 as shown in Figure 5. The cooling plate material is carbon graphite and was subjected to a power density of 300 W, which mimics the electrochemical behavior of a PEMFC [22]. The power density was then converted to a heat flux value by dividing it with the surface area heater pad resulting value of 6493.5 W/m². Meanwhile, the number of meshing elements used was also observed as it is an important factor in ensuring the optimum data analysis duration [23]. As shown in Figure 5(b), the grid independence test result was conducted to identify the optimum number of meshing elements required for the analysis. It was observed that, after 2509378 meshing elements, the plate temperature value became constant showing the stability of the meshing element used. Thus, the simulation was performed for the cooling plate with 2509378 meshing elements.

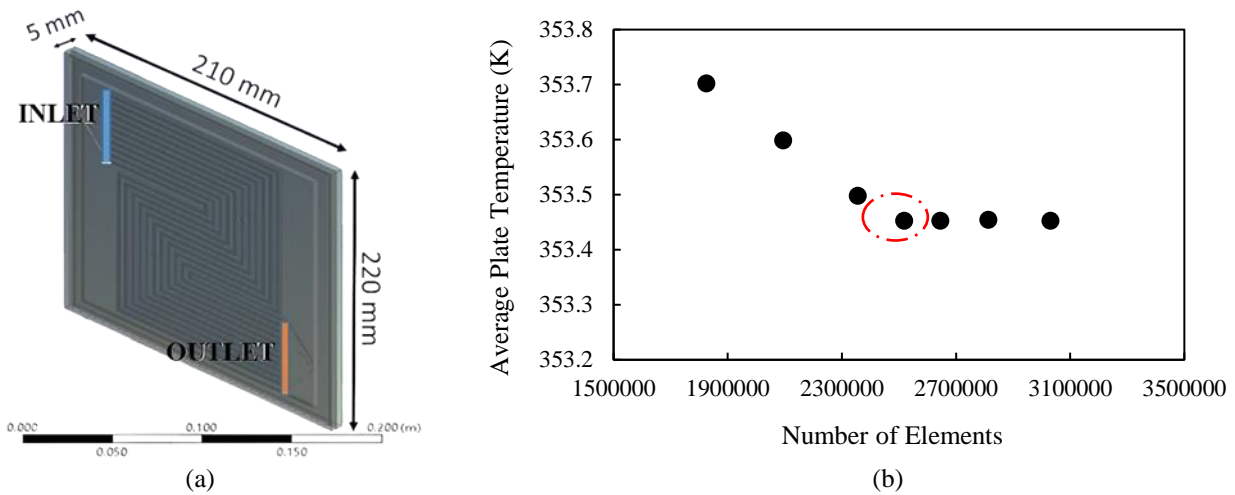


Figure 5. Cooling plate modeling Ansys Fluent: (a) geometry of the cooling plate and, (b) grid independence test

For simplification, several assumptions have been made for this ANSYS Fluent simulation [24] where the flow was considered as laminar and in steady state condition. The effect of body force was also assumed to be negligible. The fluid properties were considered constant and viscous dissipation was negligible. Since there was no relative velocity between the fluid phase and the nanoparticles which are in thermal equilibrium state, the resulting mixture can be regarded as a single phase. Finally, it was assumed that the heat transfer and fluid flow were identical for all mini channels in the serpentine cooling plate.

The governing equations for the simulation were as follows:

The continuity equation:

$$\nabla \cdot (\rho_{nf} \cdot V_m) = 0 \tag{3}$$

The momentum equation:

$$\nabla \cdot (\rho_{nf} \cdot V_m \cdot V_M) = -\nabla P + \nabla (\mu_{nf} \cdot \nabla V_m) \tag{4}$$

Fluid energy equation:

$$\nabla \cdot (\rho_{nf} \cdot V_m \cdot T) = \nabla (k_{nf} \cdot \nabla T) \tag{5}$$

Heat conduction through the solid wall:

$$0 = \nabla (k_s \cdot \nabla T_s) \tag{6}$$

No solid boundary through solid wall:

$$\vec{V} = 0 \text{ (at wall)} \tag{7}$$

In the simulation, the energy was distributed evenly across the cooling plate's bottom. Conduction moved the heat from the wall to the surface, and convection moved it throughout the fluid.

$$-k_{nf} \cdot \nabla T = q \text{ (at bottom of plate)} \tag{8}$$

$$-k_{nf} \cdot \nabla T = q \text{ (at top of plate)} \tag{9}$$

2.3.5 Mathematical model for heat transfer and fluid flow analysis

The heat transfer coefficient was calculated using the following equation:

$$h = \frac{q}{T_{Plate} - \left(\frac{T_i + T_o}{2}\right)} \tag{10}$$

where, q is the heat fluxes, W/m^2 , h is the heat transfer coefficient in $W/m^2.K$, and T_{Plate} , T_i , and T_o are temperature of plate, temperature of inlet fluid and temperature of outlet fluid respectively.

The Nusselt number was determined using the following equation:

$$Nu = \frac{hD_h}{k_{nf}} \tag{11}$$

where D_h is the hydraulic diameter, m and k_{nf} is the thermal conductivity of measured nanofluids, $W/m.K$

The pressure drops inside the cooling channel was calculated using the following equation:

$$\Delta P = P_i - P_o \tag{12}$$

where P_i and P_o are the input and output pressures, kPa, consecutively.

The pumping power was estimated using the following equation:

$$W_p = \dot{Q} \times \Delta P \tag{13}$$

where \dot{Q} is the volume flow rate, m^3/s .

The advantage ratio was then calculated using the following equation:

$$AR = \frac{h}{\Delta P} \tag{14}$$

3. RESULTS AND DISCUSSION

3.1 Nanofluids Stability

The first method employed in assessing the stability of the ternary hybrid nanofluids prepared was through visual observation as shown in Figure 6. After 15 days of preparation, the upper section of all the ternary hybrid nanofluids samples became slightly translucent, and there was slightly apparent sedimentation at the bottom of the tube. Meanwhile, after 30 days of observation, there was a slight sedimentation on the test tube's bottom, and the upper section became clearer. This sedimentation developed due to the nanoparticles in the nanofluids gradually settling due to gravitational force, dragging the particles down over time. Since the nanofluids is normally in a forced flow convection heat transfer, the suspended particles will be dissolved in the channel in its application, therefore this minimum sedimentation is deemed to be an insignificant concern in the actual application.

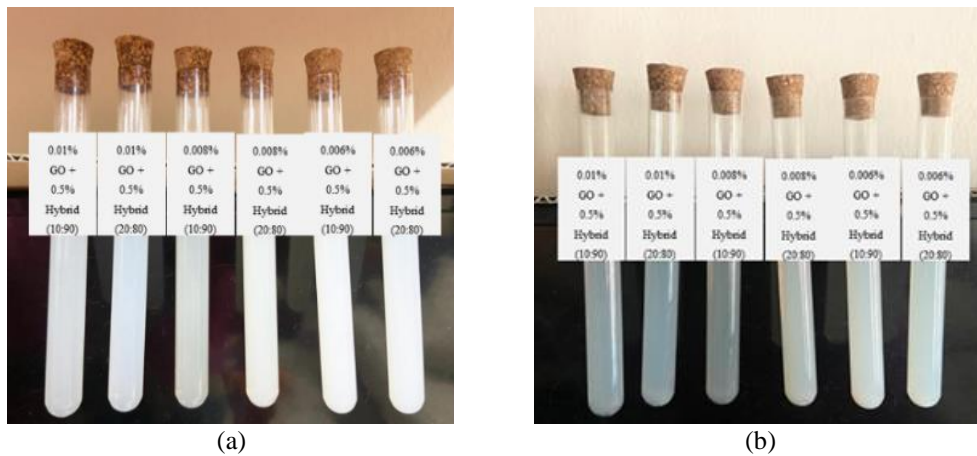


Figure 6. Visual observation: (a) after 15 days and (b) after 30 days

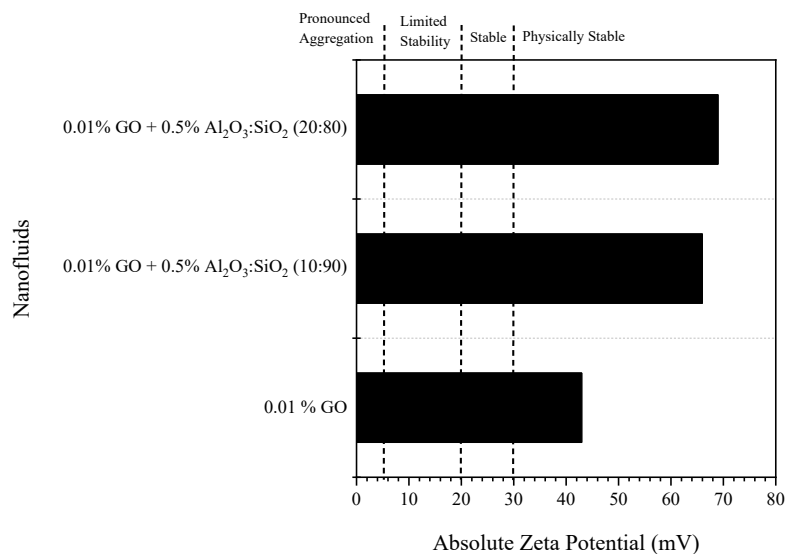


Figure 7. Zeta potential

The second method employed for stability is the zeta potential measurement. The zeta potential is referred to as excellent stability when the absolute value is over 60 mV, physical stability when the value is beyond 30 mV, stability when the value is above 20 mV, limited stability when the value is less than 20 mV, and pronounced aggregation when the value is under 5 mV [25]. In Figure 7, all the zeta potential measurements made for single 0.01 % GO nanofluids and the ternary hybrid nanofluids of 0.01% GO+ Al₂O₃: SiO₂ (10:90) and 0.01% GO+ Al₂O₃: SiO₂ (20:80) showed absolute values over 30 mV and 60 mV, indicating that the prepared 0.01% GO nanofluids sample was indeed physically stable while 0.01% GO+ Al₂O₃: SiO₂ (10:90) and 0.01% GO+ Al₂O₃: SiO₂ (20:80) were in excellent stability.

3.2. Thermophysical Properties of Nanofluids

3.2.1 Thermal conductivity

Thermal conductivity is one of the significant factors that influence the heat transfer efficiency of coolants in electrically active environments. Nanofluids that have higher thermal conductivity tend to conduct heat better and enhance the heat transfer rate. Figure 8 shows that at all concentrations, the thermal conductivity values reported for the ternary hybrid GO: Al₂O₃: SiO₂ nanofluids were higher than the base fluid. The mixture of 0.01 % GO + 0.5 % Al₂O₃: SiO₂ (20:80) with an enhancement of 1.24 % from the base fluid yielded the maximum increment for the ternary hybrid nanofluids. Meanwhile, the lowest enhancement of thermal conductivity compared to the base fluid was 0.83 % for 0.006 % GO + 0.5% Al₂O₃: SiO₂ (10:90) nanofluids. The thermal conductivity was enhanced when higher concentrations of nanoparticles were dispersed in base fluid due to the increase in Brownian motion of the suspended particles in the nanofluids [26]. Based on the result, all thermal conductivity values of the ternary hybrid nanofluids with 0.01 % GO show the highest rise from the base fluid followed by the ternary hybrid composed with 0.008 % and 0.006 % GO concentration. The increase in nanoparticle volume concentration enhanced the particle interaction and the layered structures formed by the increased particles led to a thermal bridging effect between the fluid and nanoparticle which eventually increased the thermal conductivity property.

In addition, the graph also displayed that thermal conductivity was higher in the mixture ratio of 0.01% GO + Al₂O₃: SiO₂ (20:80) nanofluids than in the 0.01% GO + Al₂O₃: SiO₂ (10:90) nanofluids. This was due to the higher thermal conductivity nanoparticle of Al₂O₃ as compared to SiO₂ [13]. In fact, Khalid et al. [8] has investigated the thermal conductivity for 0.1 % to 0.5 % Al₂O₃ and SiO₂ nanofluids and reported that Al₂O₃ nanofluids have higher thermal conductivity than SiO₂ nanofluids at all concentrations [10]. Thus, these agreements implied that increasing the mixture ratio of Al₂O₃ while reducing the ratio of SiO₂ in the ternary hybrid will enhance the thermal conductivity of the nanofluids.

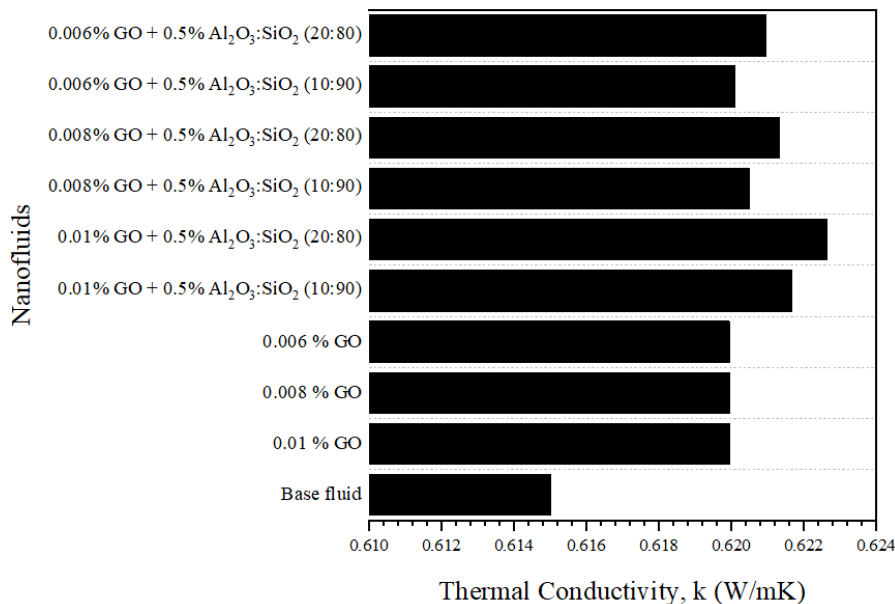


Figure 8. Thermal conductivity of nanofluids

3.2.2 Viscosity

The viscosity of the nanofluids is among the crucial aspect that needs to be considered in the application of nanofluids in cooling channels since this thermal property is directly related to the pressure drop and pumping power. The measured values of dynamic viscosity of nanofluids at various temperature ranges ranging from 30 °C to 80 °C in centipoise (cP) unit were depicted in Figure 9. The graph showed that the dynamic viscosity of mono and ternary nanofluids decreased as the temperature rose. This trend is due to the nanoparticle's Brownian motion in the nanofluids resulting in a greater transfer of energy which eventually reduces viscosity by obstructing agglomerations in the fluid at higher temperature [27].

As for the ternary hybrid nanofluids, the graph showed that the lowest viscosity value was exhibited by the 0.006 % GO + Al₂O₃: SiO₂ (20:80) with a value of 1.0284 cP which is 2.97 times higher as compared to the base fluid at 80 °C. Meanwhile, the highest viscosity value was recorded by the ternary hybrid nanofluids of 0.01% GO + Al₂O₃: SiO₂ (10:90) with a value of 1.3111 cP that yield increment up to 3.79 times higher as compared to the base fluid at 80 °C. It was observed that, as the volume concentration of nanoparticles gets higher, the nanoparticles have a stronger tendency to form larger aggregations, which increases flow resistance thus increasing the viscosity of the nanofluids. This phenomenon is associated with the attraction of van der Waals force between the particles [28]. In terms of the mixture ratios effect, the ternary hybrid nanofluids composed of 0.01% GO with a mixture of Al₂O₃: SiO₂ (10:90) recorded slightly higher enhancement of viscosity values than the ternary hybrid nanofluids composed with Al₂O₃: SiO₂ (20:80) at most of the temperature range. Sundar et al. [10] studied the viscosity of Al₂O₃ and SiO₂ nanofluids and discovered that at above 40 °C, SiO₂ nanofluid has a greater viscosity than Al₂O₃ nanofluid. The finding justified the possibility for the ternary hybrid with a lower mixture ratio of Al₂O₃ to have a greater viscosity than the ternary hybrid composed of Al₂O₃: SiO₂ (20:80) at a temperature above 40 °C.

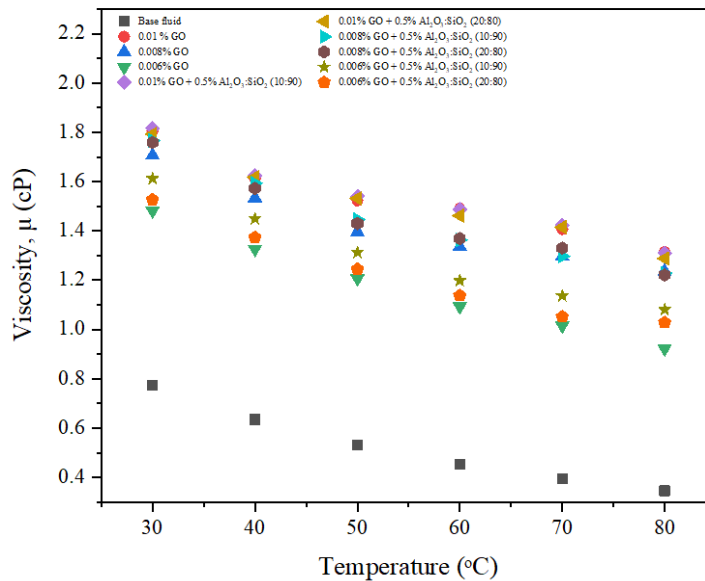


Figure 9. Viscosity of nanofluids

3.2.3 Electrical conductivity

Electrical conductivity is a measure of the capability of a material to conduct electric current. Figure 10 shows the result for the electrical conductivity of nanofluids at the different temperature ranges from 30 °C to 80 °C. The graph showed that all nanofluids measured had an increase in the value of electrical conductivity than the base fluid. In comparison to the mono GO nanofluid, the ternary hybrid recorded a tremendous increment of the electrical conductivity value. The maximum increment of electrical conductivity value recorded by the ternary hybrid nanofluid 0.01 % GO + Al₂O₃: SiO₂ (10:90) at 80 °C with the value of 173.8 μs/cm that yield increment up to 44 times larger than the base fluid, while the lowest increment value exhibited by the 0.006% GO + Al₂O₃: SiO₂ (20:80) with value of 144.7 μs/cm which recorded increment of 37 times larger than base fluid. In short, the graph indicated that at all temperature ranges, nanofluids with higher GO concentrations exhibited stronger electrical conductivity than those with lower GO concentrations. The accessibility of current conducting pathways in the nanofluid increases as GO nanoparticle concentration rises, thus increasing electrical conductivity. This finding is in good agreement with A.A. Minea [29] who reported that water-based nanofluid has higher electrical conductivity when the volume concentration increases.

On the other hand, the ternary hybrid nanofluid composed of 0.01%, 0.008%, and 0.006% GO with a mixture of Al₂O₃: SiO₂ (10:90) recorded higher enhancement of electrical conductivity values from the ternary hybrid nanofluids composed with Al₂O₃: SiO₂ (20:80) at both low and high temperature. This is well aligned with Chereches et al. [30] who experimented the electrical conductivity of simple and hybrid nanofluids containing Al₂O₃, TiO₂, and SiO₂ and found that SiO₂ yielded higher electrical conductivity values than Al₂O₃ nanofluids. Thus, lowering the ratio of Al₂O₃ while increasing the SiO₂ in the ternary hybrid nanofluid would lead to a higher electrical conductivity value.

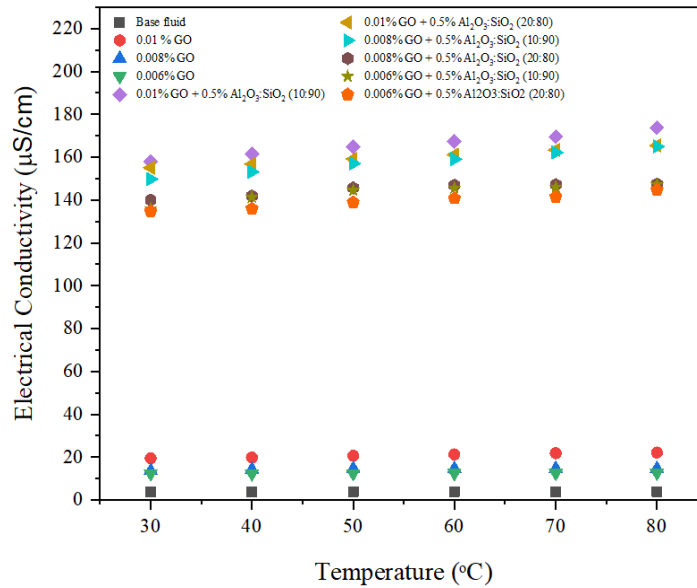


Figure 10. Electrical conductivity of nanofluids

3.3 Heat Transfer and Flow Analysis

3.3.1 Validation of simulation data

Prior to the comprehensive simulation analysis of the heat transfer and fluid flow for ternary hybrid nanofluids, the simulation for base fluid was validated with available published literature that has studied the heat transfer and fluid flow performance of the base fluid to ensure the accuracy of the simulation. Figure 11 presents a similar trend between the two data where the average plate temperature was reduced as the Reynolds number was increased [31]. The deviation of the average plate temperature was in the range of 3.48 % to 4.76 % between the simulation data and the experimental values which shows an acceptable agreement. The deviation might be due to different designs in the cooling plate used where Zakaria et al. [31] used a distributor-type cooling plate while this study was on a serpentine cooling plate.

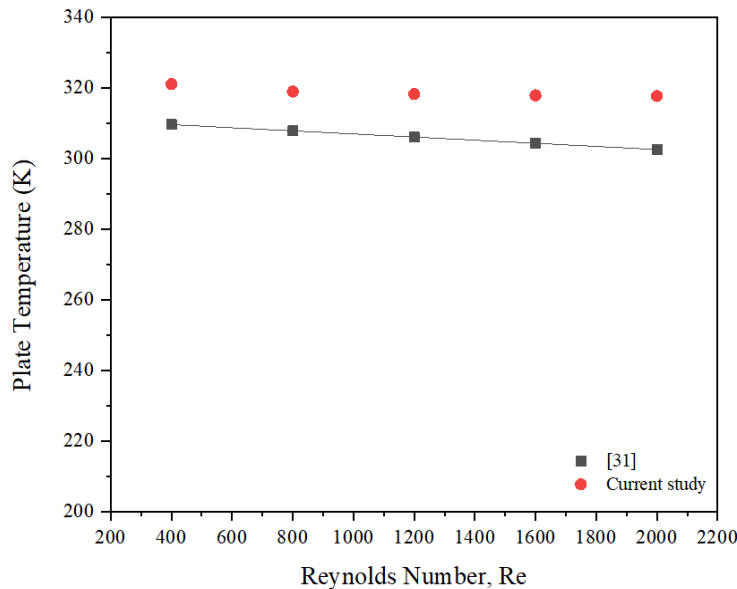


Figure 11. Validation of simulation with average temperature experimental data against [31]

3.3.2 Average plate temperature

The average plate temperature of the cooling plate for nanofluids was recorded as an indicator of the significance of nanofluids in absorbing the heat from the cooling plate. Figure 12 depicts the average plate temperature for the base fluid, mono, and ternary hybrid nanofluids. The lower the average plate temperature demonstrates that the heat is being absorbed more effectively by the coolant. Base fluid recorded the highest value of average plate temperature at all ranges of Re number. At Re 2000, 0.01 % GO + Al₂O₃: SiO₂ (10:90) nanofluid showed the highest reduction of 0.16 % followed by 0.008 % GO + Al₂O₃: SiO₂ (10:90) and 0.006 % GO + Al₂O₃: SiO₂ (10:90) with 0.15 % and 0.14 % reduction,

respectively, as compared to the base fluid. Higher values of volume concentration resulted in higher thermal conductivity thus making it easier for heat transfer to be absorbed by the nanofluids.

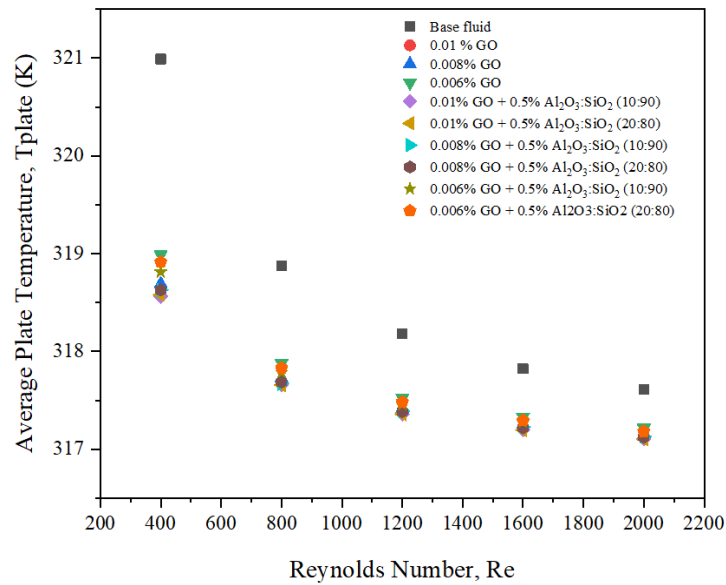


Figure 12. Average plate temperature against Reynold number

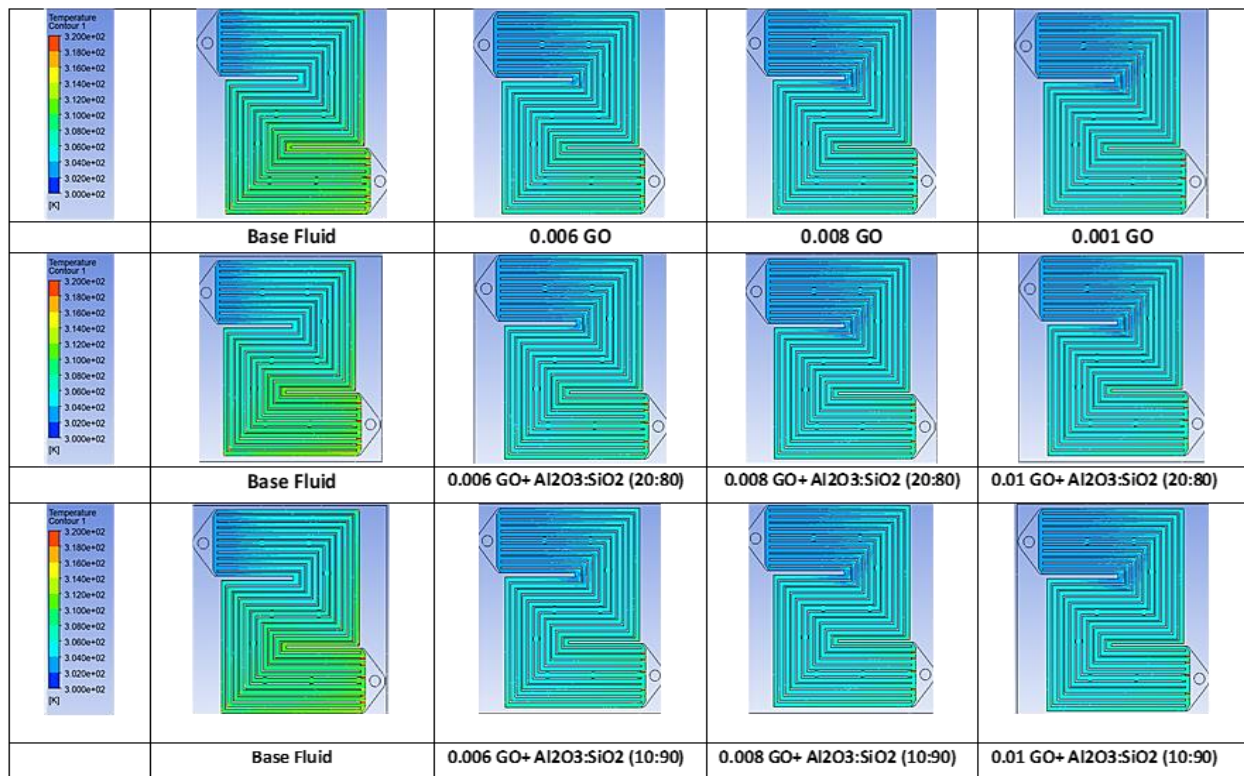


Figure 13. Cooling liquid temperature contour

The thermal behavior of the cooling plate also was then demonstrated through the fluid temperature contour. Figure 13 shows the temperature contour of the cooling liquid. All fluids displayed that the inlet area is relatively colder than the outlet area. This condition indicates that all fluids absorbed heat from the cooling plate which led to a rise in temperature as the fluid flowed through the outlet. All measured nanofluids demonstrated colder temperature gradients compared to the base fluid. This indicates enhancement of the heat transfer as the cooling plate reduces in temperature resulting in a lower temperature of flowing fluid on the plate. Meanwhile, the contour of the mono GO and the ternary hybrid is almost similar due to very small temperature differences in terms of average plate temperature. When the volume concentration of GO in the mono and ternary hybrid nanofluid increased, the blue region occupied a bigger area while the green color slowly disappeared. This implies that increasing the volume of concentration improves the heat transfer which causes a reduction of the temperature of the cooling plate which eventually leads to a lower temperature range of

the fluid flowing on the plate. This finding is well-aligned with the result of the coolant temperature contour obtained by Zakaria et al. [24] who also studied the behavior of nanofluid in a serpentine cooling plate.

3.3.3 Heat transfer coefficient

The heat transfer coefficient is a crucial parameter that defines the heat transfer rate between fluid or any other medium across a surface. It demonstrated the competency of the fluid or medium to conduct heat and can be translated as the quantity of heat transferred per unit area and difference in temperature. The heat transfer coefficient of a coolant is generally influenced by the thermophysical properties of the fluid, fluid regime and flow rate, and geometry or nature of the surface [27]. Figure 14 displays the heat transfer coefficient for all the measured nanofluids. All the mono and ternary hybrid nanofluids recorded enhancement of heat transfer coefficient as compared to the base fluid. It was observed that heat transfer coefficient was influenced by volume % concentration as the highest heat transfer coefficient value was exhibited by the ternary hybrid nanofluid 0.01% GO + Al₂O₃: SiO₂ (10:90) with a value of 11484.3 W/m² K at Re 2000. This was equivalent to 1.086 times higher than the base fluid. This was then followed by 0.01% GO + Al₂O₃: SiO₂ (20:80) with 1.063 times higher than the base fluid. The higher content of nanoparticles in these nanofluids boosted the heat transfer rate coefficient due to their higher thermal conductivity characteristics as compared to the base fluid [32]. A similar pattern was also reported by Hwang et al. [33] that the water-based Al₂O₃ increased the heat transfer coefficient by 8 % when the volume concentration of the nanofluid was raised from 0.01 % to 0.3 %.

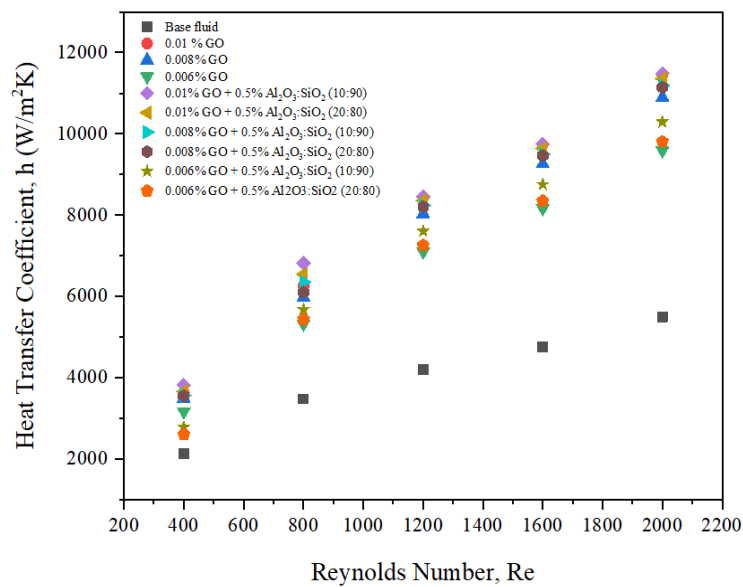


Figure 14. Heat transfer coefficient against Reynolds number

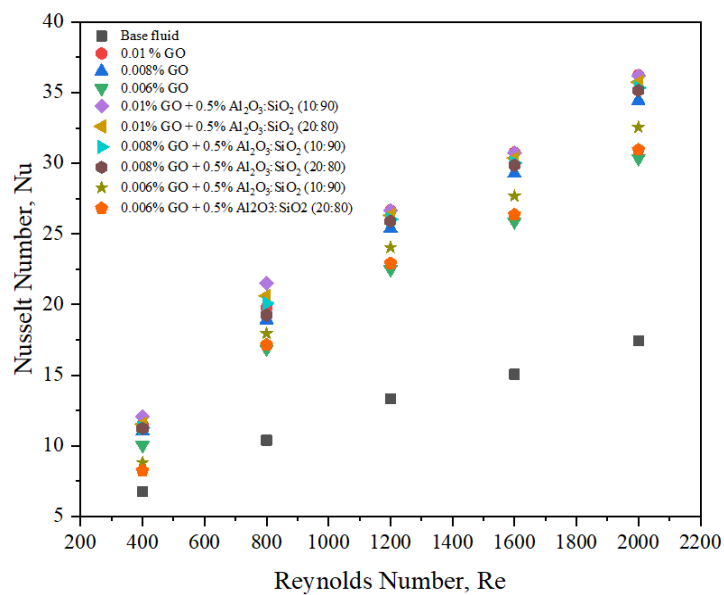


Figure 15. Nusselt number against Reynolds number

3.3.4 Nusselt Number

The Nusselt number is a dimensionless parameter that measures the ratio of convective heat transfer over conductive heat transfer. Figure 15 displayed that all measured mono and ternary hybrid nanofluids recorded higher Nusselt numbers than the base fluid. The base fluid has the lowest Nusselt number of 17.42 at Re 2000, whereas the ternary hybrid nanofluid with 0.01% GO + Al₂O₃: SiO₂ (10:90) had the greatest value of 36.2. This improvement is equivalent of 107% as compared to base fluid. This is due to the improved heat transfer coefficient values of nanofluids as compared to base fluid. The ternary hybrid nanofluids rank was the top one, followed by the mono nanofluids. The results also showed that nanofluids with the highest GO content has the greatest increase in Nusselt number as compared to those with lower GO concentration at all ranges of Re number. The increase in volume concentrations led to an increase in thermal conductivity which consequently enhance the heat transfer coefficient and Nusselt number, which is in good agreement with result of Muhammad et al. [34].

3.3.5 Pressure drop

The hydraulic performance of the nanofluid in the cooling channel was represented by the pressure drop value which was the differences between the inlet pressure and the outlet pressure. Figure 16 displayed the pressure drop resulted from the nanofluids at various ranges of Re number. At Re 2000, the highest-pressure drop was recorded by the ternary hybrid nanofluid 0.01% GO + Al₂O₃: SiO₂ (10:90) with the value of 25.9 kPa, which is equivalent to 5.5 times higher than the base fluid. This was then followed by 0.01% GO + Al₂O₃: SiO₂ (20:80) with 5.3 times increment over base fluid. This was mainly due to the higher value of viscosity of the ternary hybrid nanofluids as compared to the base fluid. The addition of nanoparticles to the base fluid caused the clustering due to the attraction of van der Waals force between the particles which consequently increase the viscosity [28]. The findings also demonstrated that across all Re number ranges, nanofluids with the highest GO content exhibited a greater rise in pressure drop than those with lower GO concentrations. At Re 400, for example, 0.01% GO + Al₂O₃: SiO₂ (20:80) nanofluid recorded the highest pressure drop, at 449.2 %, over the base fluid, followed by 0.008 % GO + Al₂O₃: SiO₂ (20:80) and 0.006% GO + Al₂O₃: SiO₂ (20:80), with 414.9 % and 288 % enhancement, respectively. As the volume concentration of nanoparticles gets higher, the nanoparticles have a stronger tendency to form larger aggregations, which increases flow resistance and, as a result, the viscosity of the nanofluids.

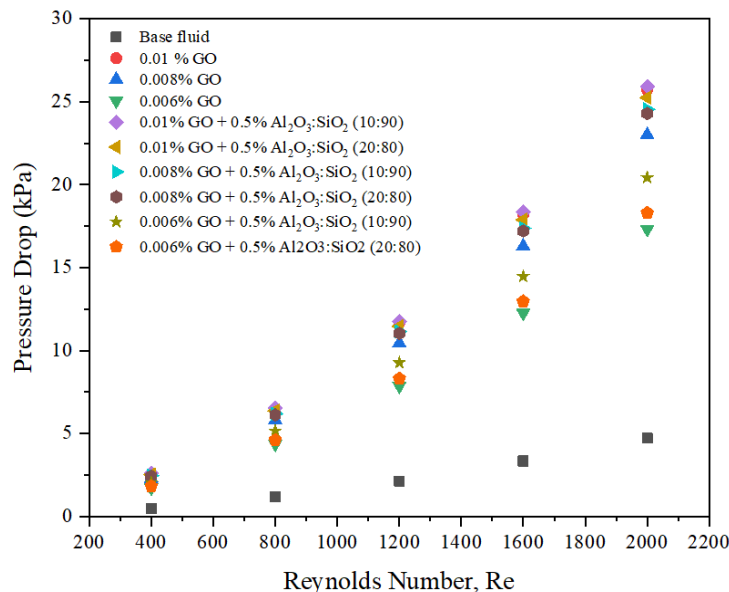


Figure 16. Pressure Drop against Reynolds number

3.3.6 Pumping Power

The pressure drop then translated to pumping power to further analyze the effect of the mono GO and GO: Al₂O₃: SiO₂ nanofluids on the fluid flow. Figure 17 depicts the pumping power for the base fluid and nanofluids. The base fluid recorded the lowest pumping power as compared to the mono and ternary hybrid nanofluids. At Re 2000, the minimum pumping power was recorded by the base fluid with the value of 0.182 W, whereas the maximum pumping power was exhibited by 0.01 % GO + Al₂O₃: SiO₂ (10:90) nanofluids with pumping power of 2.335 W. The results also showed that across all Re number ranges, the ternary hybrid nanofluids containing greater GO levels experienced an additional pumping power than ternary hybrid nanofluids with lower GO concentrations for both lower and higher Re numbers. At Re 1200, for example, 0.01 % GO + Al₂O₃: SiO₂ (10:90) nanofluid recorded the highest pumping power, at 1184 % over the base fluid, followed by 0.008 % GO + Al₂O₃: SiO₂ (10:90) and 0.006% GO + Al₂O₃: SiO₂ (10:90), with 1083 % and 798 % enhancement, respectively. This finding is aligned with Louis et al. [35] who also reported that the fluid viscosity increased up to 2.03% when the concentration of nanofluid in the base fluid increased from 0.0 % to 0.8 %, thus resulting

in greater pumping power to cover up the losses caused by the higher pressure drop. In terms of mixture ratio, all the ternary hybrid nanofluid with the mixture of Al_2O_3 : SiO_2 (10:90) led to a greater pumping power than all the ternary hybrid nanofluid made with Al_2O_3 : SiO_2 (20:80). This is true to all volume concentration of GO added to the Al_2O_3 : SiO_2 nanofluids. This was due to the higher viscosity value of the 20:80 mixture as compared to 10:90, which was similar to findings reported by Khalid et al. [13].

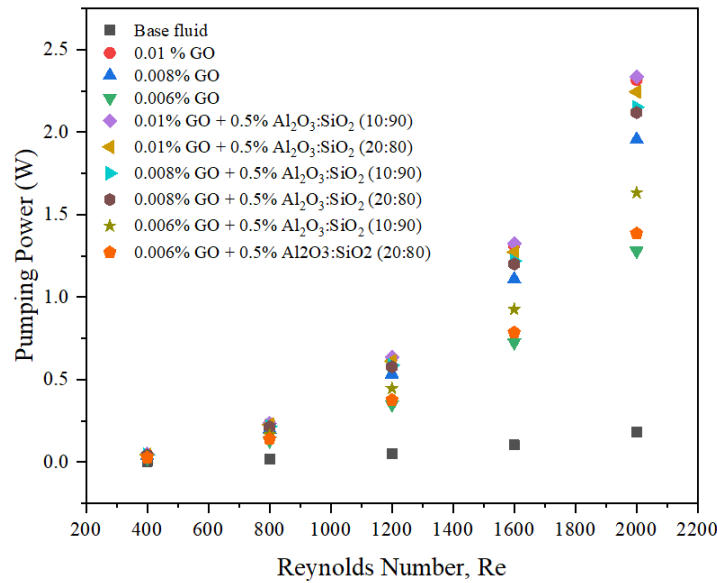


Figure 17. Pumping power against Reynolds number

3.3.7 Advantage ratio

In summary, the effect of hybridizing the GO: Al_2O_3 : SiO_2 to form a novel ternary hybrid nanofluid resulted in the enhancement of its critical thermo-physical properties which are thermal conductivity, and viscosity. These properties were then applied to a serpentine cooling plate to review the heat transfer improvement. However, the heat transfer enhancement of these properties was coupled with penalties as the increase of the viscosity led to higher pressure drop and pumping power. To confirm the feasibility of the GO: Al_2O_3 : SiO_2 ternary hybrid nanofluids, the advantage ratio of heat transfer coefficient over pressure losses is measured. The nanofluids are considered feasible if the measured advantage ratio is equal to or greater than 1 [36]. Figure 18 demonstrates that the base fluid consistently exhibits advantage ratios larger than 1 over the entire range of Re values. Meanwhile, mono and ternary hybrid nanofluids, on the other hand, only showed advantages higher than 1 in the lower Re area within the range of Re 400 to 800. The highest advantage ratio for the ternary hybrid nanofluids was recorded by the 0.01% GO + Al_2O_3 : SiO_2 (10:90) with a value of 1.47 at Re 400.

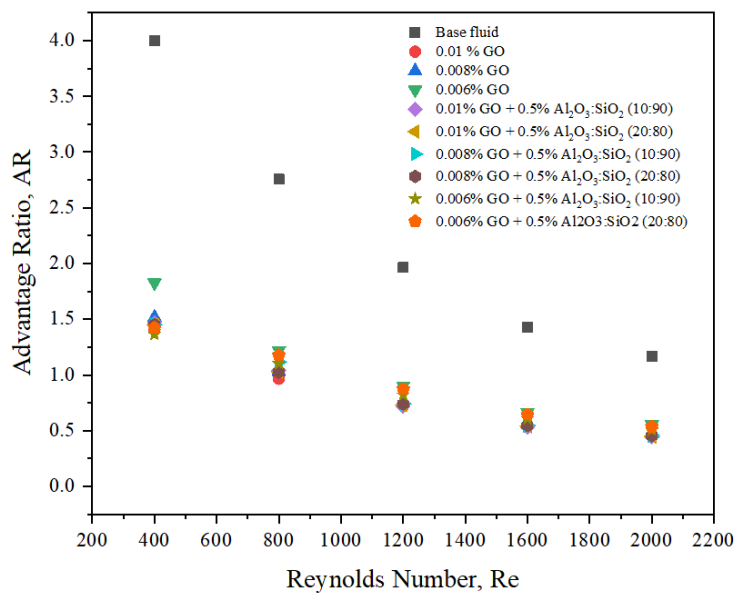


Figure 18. The advantage ratio

Meanwhile, the lowest advantage ratio at Re 400 was exhibited by 0.006% GO + Al_2O_3 : SiO_2 (10:90) with a value of 1.36. The highest advantage ratio for the ternary hybrid nanofluids by the 0.01% GO + Al_2O_3 : SiO_2 (10:90) was due to

its higher enhancement in terms of heat transfer coefficient as compared to the pressure drop penalty. However, at the higher Re region than Re 800, the advantage ratio of both mono and ternary hybrid nanofluids dropped to below 1, thus indicating the insignificance of practical application. In addition to that, the properties of the nanofluid used in this study were measured at 30 °C whereby in the real-world application, the feasibility of the novel nanofluid can be further improved by operating at a slightly higher operating temperature as the viscosity tends to decrease as the temperature increases, which reduce the pressure drop penalty.

4. CONCLUSIONS

The thermophysical properties of thermal conductivity, electrical conductivity, and dynamic viscosity of GO: Al₂O₃: SiO₂ ternary hybrid nanofluids were presented in this study. The highest enhancement of thermal conductivity was made by 0.001% GO + 0.5% Al₂O₃: SiO₂ (20:80) with an enhancement of 1.24% from the base fluid. The maximum value of viscosity was recorded by 0.01% GO + Al₂O₃: SiO₂ (10:90) at 80 °C yielded 3.79 times higher compared to the base fluid. Meanwhile, the minimum increment value of electrical conductivity exhibited ternary hybrid nanofluid 0.01% GO + Al₂O₃: SiO₂ (10:90) at 80 °C with the value of 173.8 μs/cm that yield increment up to 44 times larger than the base fluid. In term of its application in a serpentine cooling plate, the heat transfer and fluid flow performance of the GO: Al₂O₃: SiO₂ ternary hybrid nanofluids in a serpentine cooling plate using showed better heat transfer performance as compared to the base fluid and mono GO nanofluids. The 0.01% GO + Al₂O₃: SiO₂ (10:90) nanofluid, has a greater value of heat transfer coefficient than the 0.01% GO + Al₂O₃: SiO₂ (20:80). As for the fluid flow analysis, due to the significant effect of the viscosity value, the GO: Al₂O₃: SiO₂ ternary hybrid nanofluids has resulted in the higher pressure drop across the cooling plate which eventually led to the higher pumping power required to cater the pressure losses. In terms of its feasibility for adoption, the advantage ratio was beneficial at lower Re number of Re 400 to Re 800. However, further experimental studies are required to validate these findings.

ACKNOWLEDGMENTS

The authors would like to acknowledge Geran Insentif Penyelidikan, Universiti Teknologi MARA (UiTM) [600-RMC/GIP 5/3(119/2023)], and College of Engineering, Universiti Teknologi MARA for research grants and funding.

CONFLICT OF INTEREST

All authors declare that they have no conflicts of interest

AUTHORS CONTRIBUTION

The authors confirm the equal contribution in each part of this work. All authors reviewed and approved the final version of this work.

F. M. Hanapiah (Conceptualization; Methodology; Formal analysis; Visualisation; Writing - original draft)

I. A. Zakaria (Conceptualization; Methodology; Formal analysis; Visualisation; Writing - original draft)

S. R. Makhzin (Conceptualization; Methodology; Formal analysis; Visualisation)

N. Hamzan (Conceptualization; Methodology; Formal analysis; Visualisation)

REFERENCES

- [1] T. Balaji, C. Selvam, D. M. Lal, "A review on electronics cooling using nanofluids," in *IOP Conference Series: Materials Science and Engineering*, vol. 1130, no. 1, p. 012007, 2021.
- [2] G. Colangelo, E. Favale, M. Milanese, A. de Risi, D. Laforgia, "Cooling of electronic devices: Nanofluids contribution," *Applied Thermal Engineering*, vol. 127, pp. 421-435, 2017.
- [3] D. Saidina, M. Abdullah, M. Hussin, "Metal oxide nanofluids in electronic cooling: A review," *Journal of Materials Science: Materials in Electronics*, vol. 31, no. 6, pp. 4381-4398, 2020.
- [4] M. Bahiraei, S. Heshmatian, "Electronics cooling with nanofluids: A critical review," *Energy Conversion and Management*, vol. 172, pp. 438-456, 2018.
- [5] M. Awais, N. Ullah, J. Ahmad, F. Sikandar, M. M. Ehsan, S. Salehin, et al., "Heat transfer and pressure drop performance of Nanofluid: A state-of-the-art review," *International Journal of Thermofluids*, vol. 9, p. 100065, 2021.
- [6] A. Afzal, S. J. Ukkund, "Experimental investigation on physical and thermal properties of graphite nanofluids," in *AIP conference proceedings*, vol. 2039, no. 1, 2018.
- [7] M. S. Kamel, O. Al-Oran, F. Lezsovits, "Thermal conductivity of Al₂O₃ and CeO₂ nanoparticles and their hybrid based water nanofluids: An experimental study," *Periodica Polytechnica Chemical Engineering*, vol. 65, no. 1, pp. 50-60, 2021.
- [8] S. Khalid, I. A. Zakaria, W. A. N. Wan Mohamed, "Comparative analysis of thermophysical properties of Al₂O₃ and SiO₂ nanofluids," *Journal of Mechanical Engineering*, vol. 8, no. 1, pp. 153-163, 2019.

- [9] S. Suresh, K. Venkitaraj, P. Selvakumar, M. Chandrasekar, "Effect of Al_2O_3 -Cu/water hybrid nanofluid in heat transfer," *Experimental Thermal and Fluid Science*, vol. 38, pp. 54-60, 2012.
- [10] L. S. Sundar, K. V. Sharma, M. K. Singh, A. Sousa, "Hybrid nanofluids preparation, thermal properties, heat transfer and friction factor—A review," *Renewable and Sustainable Energy Reviews*, vol. 68, pp. 185-198, 2017.
- [11] G. M. Moldoveanu, C. Ibanescu, M. Danu, A. A. Minea, "Viscosity estimation of Al_2O_3 , SiO_2 nanofluids and their hybrid: An experimental study," *Journal of Molecular Liquids*, vol. 253, pp. 188-196, 2018.
- [12] G. M. Moldoveanu, G. Huminic, A. A. Minea, A. Huminic, "Experimental study on thermal conductivity of stabilized Al_2O_3 and SiO_2 nanofluids and their hybrid," *International Journal of Heat and Mass Transfer*, vol. 127, pp. 450-457, 2018.
- [13] S. Khalid, I. Zakaria, W. H. Azmi, W. A. N. W. Mohamed, "Thermal—electrical—hydraulic properties of Al_2O_3 - SiO_2 hybrid nanofluids for advanced PEM fuel cell thermal management," *Journal of Thermal Analysis and Calorimetry*, vol. 143, pp. 1555-1567, 2020.
- [14] A. Ramadhan, W. Azmi, R. Mamat, K. Hamid, S. Norsakinah, "Investigation on stability of tri-hybrid nanofluids in water-ethylene glycol mixture," in *IOP Conference Series: Materials Science and Engineering*, vol. 469, p. 012068, 2019.
- [15] N. A. S. Muzaidi, M. A. Fikri, K. N. S. Wan Salihin Wong, A. Z. Mohammad Sofi, R. Mamat, N. Mohd Adenam, et al., "Heat absorption properties of $\text{CuO}/\text{TiO}_2/\text{SiO}_2$ trihybrid nanofluids and its potential future direction towards solar thermal applications," *Arabian Journal of Chemistry*, vol. 14, no. 4, p. 103059, 2021.
- [16] U. García-Vidal, J. L. Jiménez-Pérez, G. López-Gamboa, R. Gutiérrez-Fuentes, J. F. Sánchez-Ramírez, Z. N. Correa-Pacheco, et al., "Synthesis of compact and porous SiO_2 nanoparticles and their effect on thermal conductivity enhancement of water-based nanofluids," *International Journal of Thermophysics*, vol. 44, no. 6, pp. 1-20, 2023.
- [17] S. Zainon, W. Azmi, "Recent progress on stability and thermo-physical properties of mono and hybrid towards green nanofluids," *Micromachines*, vol. 12, no. 2, p. 176, 2021.
- [18] S. Zainon, W. Azmi, "Stability and thermo-physical properties of green bio-glycol based TiO_2 - SiO_2 nanofluids," *International Communications in Heat and Mass Transfer*, vol. 126, p. 105402, 2021.
- [19] Y. Gao, Y. Xi, Y. Zhenzhong, A. P. Sasmito, A. S. Mujumdar, L. Wang, "Experimental investigation of specific heat of aqueous graphene oxide Al_2O_3 hybrid nanofluid," *Thermal Science*, vol. 25, no. 1 Part B, pp. 515-525, 2021.
- [20] R. Taherialekouhi, S. Rasouli, A. Khosravi, "An experimental study on stability and thermal conductivity of water-graphene oxide/aluminum oxide nanoparticles as a cooling hybrid nanofluid," *International Journal of Heat and Mass Transfer*, vol. 145, p. 118751, 2019.
- [21] W. Guo, G. Li, Y. Zheng, C. Dong, "Measurement of the thermal conductivity of SiO_2 nanofluids with an optimized transient hot wire method," *Thermochimica Acta*, vol. 661, pp. 84-97, 2018.
- [22] X. Chen, Q. Liu, Y. Fang, L. He, T. Huang, Y. Zhang, et al., "Numerical study of a MIMO-shaped cooling plate in PEMFC stack for heat transfer enhancement," *Energy reports*, vol. 7, pp. 5804-5814, 2021.
- [23] M. Lee, G. Park, C. Park, C. Kim, "Improvement of grid independence test for computational fluid dynamics model of building based on grid resolution," *Advances in Civil Engineering*, vol. 2020, pp. 1-11, 2020.
- [24] I. A. Zakaria, W. A. N. Wan Mohamed, A. Mohd Ihsan Mamat, K. I. Sainan, M. R. Mat Nawi, G. H. Najafi, "Numerical analysis of Al_2O_3 nanofluids in serpentine cooling plate of PEM fuel cell," *Journal of Mechanical Engineering*, vol. 5, no. 1, pp. 1-13, 2018.
- [25] K. Cacia, F. Ordoñez, C. Zapata, B. Herrera, E. Pabón, R. Buitrago-Sierra, "Surfactant concentration and pH effects on the zeta potential values of alumina nanofluids to inspect stability," *Colloids and Surfaces A: Physicochemical and Engineering Aspects*, vol. 583, p. 123960, 2019.
- [26] M. Gupta, V. Singh, R. Kumar, Z. Said, "A review on thermophysical properties of nanofluids and heat transfer applications," *Renewable and Sustainable Energy Reviews*, vol. 74, pp. 638-670, 2017.
- [27] K. Apmann, R. Fulmer, B. Scherer, S. Good, J. Wohld, S. Vafaei, "Nanofluid heat transfer: enhancement of the heat transfer coefficient inside microchannels," *Nanomaterials*, vol. 12, no. 4, p. 615, 2022.
- [28] S. Zhang, X. Han, "Effect of different surface modified nanoparticles on viscosity of nanofluids," *Advances in Mechanical Engineering*, vol. 10, no. 2, p. 1687814018762011, 2018.
- [29] A. A. Minea, "A review on electrical conductivity of nanoparticle-enhanced fluids," *Nanomaterials*, vol. 9, no. 11, p. 1592, 2019.
- [30] E. I. Chereches, A. A. Minea, "Electrical conductivity of new nanoparticle enhanced fluids: An experimental study," *Nanomaterials*, vol. 9, no. 9, p. 1228, 2019.

- [31] I. A. Zakaria, W. A. N. W. Mohamed, M. B. Zailan, W. H. Azmi, "Experimental analysis of SiO₂-Distilled water nanofluids in a Polymer Electrolyte Membrane fuel cell parallel channel cooling plate," *International Journal of Hydrogen Energy*, vol. 44, no. 47, pp. 25850-25862, 2019.
- [32] F. C. Nagarajan, S. Kannaiyan, C. Boobalan, "Intensification of heat transfer rate using alumina-silica nanocoolant," *International Journal of Heat and Mass Transfer*, vol. 149, p. 119127, 2020.
- [33] K. S. Hwang, S. P. Jang, S. U. Choi, "Flow and convective heat transfer characteristics of water-based Al₂O₃ nanofluids in fully developed laminar flow regime," *International journal of heat and mass transfer*, vol. 52, no. 1-2, pp. 193-199, 2009.
- [34] N. M. a. Muhammad, N. A. C. Sidik, A. Saat, B. Abdullahi, "Effect of nanofluids on heat transfer and pressure drop characteristics of diverging-converging minichannel heat sink," *CFD Letters*, vol. 11, no. 4, pp. 105-120, 2019.
- [35] S. P. Louis, S. Ushak, Y. Milian, M. Nemés, A. Nemés, "Application of nanofluids in improving the performance of double-pipe heat exchangers—A critical review," *Materials*, vol. 15, no. 19, p. 6879, 2022.
- [36] W. Azmi, K. Sharma, P. Sarma, R. Mamat, S. Anuar, "Comparison of convective heat transfer coefficient and friction factor of TiO₂ nanofluid flow in a tube with twisted tape inserts," *International Journal of Thermal Sciences*, vol. 81, pp. 84-93, 2014.